Preprints of the 19th World Congress
The International Federation of Automatic Control
Cape Town, South Africa. August 24-29, 2014

Towards load control of populations of air conditioners with guaranteed comfort margins

Nariman Mahdavi [*,**] **Cristian Perfumo** [*]
Julio H. Braslavsky [*,**]

[*] *CSIRO Energy Technology, PO Box 330, Newcastle, NSW 2300 Australia.* {*nariman.mahdavimazdeh, cristian.perfumo, julio.braslavsky*}*@csiro.au*
[**] *School of EECS, The University of Newcastle, Newcastle, Australia*

Abstract: The increasing penetration of renewable sources in electricity grids has motivated interest in controlling loads to compensate for variability of these generation sources. Air conditioners (ACs) are one type of loads that can be effectively controlled by broadcasting temperature setpoint offsets and using measurements of aggregate power demand for feedback, as shown in recent works. While such control approach can arbitrarily shape demand, it does so at the expense of end-use comfort, which may be a deterrent to participation in such programmes. This paper explores the use of an alternative to setpoint offsets to shape aggregate demand of ACs without violating end-use comfort levels. The proposed control consists in manipulating the width of the ACs' temperature regulation bands by raising the low temperature limit (or lowering the high temperature limit) to change aggregate demand while keeping AC temperatures within the specified ranges. We develop a deterministic mathematical model for the AC aggregate demand response to changes in the new proposed control input, and numerically validate it against a simulated population of ACs. The resulting model is amenable to systematic analysis and design for direct load control with guaranteed comfort margins. We illustrate this point by deriving a theoretical upper bound on the maximum energy that may be released from a given population of ACs controlled using the proposed control input.

1. INTRODUCTION

Electric loads such as air conditioners (ACs) and other thermostatically-controlled loads (TCLs) are suitable for direct load control at the residential level due to two main characteristics. Firstly, thanks to the intrinsic thermal inertia of the AC spaces, brief perturbations to the ACs steady state operation can be made with small or no measurable impact to comfort levels. Secondly, these loads can generate a rapid collective response to simple external control signals, such as the introduction of small temperature setpoint offsets, used by utilities in thermostat setback load control programs (Callaway and Hiskens, 2011). Direct load control (DLC) of ACs can effectively provide energy services such as load shifting to reduce peaks in demand, and load following to mitigate high variability in renewable energy generation (Callaway, 2009; Hughes, 2010; Perfumo et al., 2012; Bashash and Fathy, 2013; Zhang et al., 2013; Braslavsky et al., 2013).

The introduction of small offsets in temperature setpoints is simple to implement and can achieve tight control of the aggregate demand of AC populations. However, with this approach demand control comes at the expense of user comfort, which, while it may be moderated by careful monitoring, could be a deterrent to participation in programmes implementing such DLC strategy.

This paper investigates an alternative to shape aggregate power demand in populations of ACs *without affecting end-use comfort*. The proposed control manipulates the *width* of the ACs temperature regulation deadbands (centred around temperature setpoints) by independently shifting its boundaries while keeping temperatures within the original limits. Naturally, the extent to which the proposed manipulated variable can shift aggregate demand is limited by the widths of the regulation bands and their minimum admissible values to avoid equipment damage. Provided such limits are respected, the proposed control input opens a new avenue for model-based DLC design with guaranteed margins of end-use performance.

Our main technical contribution is a mathematical model for the dynamic aggregate demand response of a population of ACs to one-sided step changes to temperature regulation bands. This model extends a model introduced in Perfumo et al. (2012) to incorporate the new proposed control input. The model is a second-order linear time invariant approximation of the response, which, as that in Perfumo et al. (2012), is analytically parametrized by the distributed physical characteristics of the population. In contrast to the model obtained in Perfumo et al. (2012), however, the present model is nonlinear in the new control input. These nonlinearities, however, are tractable and amenable to control analysis and design techniques for the range of input values of practical relevance. We illustrate the latter point by computing a theoretical upper bound on the maximum amount of energy that may be released by DLC of a population of ACs without violating user-

specified comfort levels when the proposed control input is applied. The proposed model is validated for a range of admissible input values against responses of a simulated heterogeneous population of 10,000 ACs.

An alternative to achieve DLC of TCLs with no impact to end-use performance is introduced in Li et al. (2010) as a decentralised control algorithm where each device plans its own cooling/heating cycling sequence so that the temperature is maintained within a specified band. The aggregate power consumption is adjusted to a centrally broadcast cap. In comparison to the approach in the present paper, the decentralised scheme in Li et al. (2010) requires the ACs to have two-way communications to adjust their planning in real-time, while our controller can be implemented over one-way communications using feedback from feeder measurements Braslavsky et al. (2013).

Furthermore, a centralised DLC approach in Zhang et al. (2013) shows how nondisruptive peak shaving can be obtained via a probabilistic control signal numerically computed by inverting an accurate model of the population aggregate demand response. While such model accounts for compressor delays and detailed thermal dynamics (neglected in the present paper), it comprises potentially hundreds of states, which makes the mathematical analysis of transient responses more challenging. The model proposed in the present paper is of order two and yet it captures the essential aggregate dynamics required for accurate transient analysis and DLC using simple controllers that can be systematically tuned.

2. SYSTEM AND PRELIMINARY ANALYSIS

We now define the system under consideration, namely a population of ACs that independently regulate their temperatures using thermostat-based on-off controllers. We consider a DLC strategy based on manipulating the width of the thermostat deadbands as a means to control aggregate demand, assuming that the upper and lower limits of the deadbands may be independently changed in real time. We show how small offsets to these values changes can be effective in manipulating aggregate demand while keeping end-use function within the specified temperature limits, in contrast with control strategies based on introducing temperature setpoint offsets (e.g. Callaway, 2009; Bashash and Fathy, 2013; Perfumo et al., 2012; Mathieu et al., 2013), where DLC comes at the expense of shifting defined end-use comfort constraints.

The dynamics of each AC operating independently in the population may be described by the differential equation with switching feedback (e.g., Ihara and Schweppe, 1981)

$$\dot{\theta}_i(t) = -(C_i R_i)^{-1} \left[\theta_i(t) - \theta_a + m_i(t) R_i P_i + w(t)\right] \quad (1)$$

$$m_i(t^+) = \begin{cases} 0 & \text{if } \theta_i(t) \leq \theta_- + \alpha(t) \\ 1 & \text{if } \theta_i(t) \geq \theta_+ + \beta(t) \\ m_i(t) & \text{otherwise,} \end{cases} \quad (2)$$

where the continuous state $\theta_i(t)$ is the regulated temperature for the i-th AC, $i \in \{1, 2, \ldots, n\}$, and the discrete state $m_i(t)$ is the state of its relay, which switches the compressor on and off with the hysteretic control rule (2). The inputs $\alpha(t)$ and $\beta(t)$ are the proposed offsets to the lower and upper limits of the relay deadband.

The relay control law (2) maintains the temperature $\theta_i(t)$ oscillating within the hysteresis deadband $[\theta_- + \alpha(t), \theta_+ + \beta(t)]$ with a period that is a function of the width of this deadband, the thermal capacitance (kWh/° C) and thermal resistance (^oC/kW) of the room, C_i and R_i, and the thermal power P_i (kW) of the AC. The input $w(t)$ is a random variable representing thermal disturbances.

The normalised aggregate demand $D(t)$ of a population of n ACs independently operating with the dynamics (1)-(2) is given by the ratio

$$D(t) = \frac{\sum_{i=1}^{n} m_i(t) \frac{P_i}{\mathrm{COP}_i}}{\sum_{i=1}^{n} \frac{P_i}{\mathrm{COP}_i}}, \quad (3)$$

where COP_i is the coefficient of performance of the ith AC. The COP is in general a function of the difference $\theta_a - \theta_i(t)$, but for simplicity will be assumed constant in this paper. The normalising factor $\sum_{i=1}^{n} \frac{P_i}{\mathrm{COP}_i}$ in (3) represents the maximum demand when all the ACs have their compressors switched on. This is the maximum power that could be shed from the population by DLC.

Equation (3) may be used to study aggregate demand dynamics numerically, assuming the distributed parameters C_i, R_i, P_i are known. By simulating an array of n independent sets of Equations (1)-(2) coupled by Equation (3) one can analyse the effects of ambient temperature, parameter distribution, and changes in temperature set-points (Perfumo et al., 2013). We use such approach to numerically validate the proposed reduced-order model on a simulated population of 10,000 ACs with distributed parameters randomly sampled according to Table 1.

Table 1. Simulation parameters.

Parameter	Mean value	Description
R	2 °C/kW	Thermal resistance (log-normally distributed).
C	3.6 kWh/°C	Thermal capacitance (log-normally distributed).
P	6 kW	Thermal power (log-normally distributed).
θ_-	19.5 °C	Lower end of hysteresis band.
θ_+	20.5 °C	Higher end of hysteresis band.
θ_a	26 °C	Ambient temperature.
σ_{rel}	0.2	Standard deviation of log-normal distributions as a fraction of the mean value for R, C and P.

In the rest of the paper we focus on the lower end of the temperature deadband $\alpha(t)$. The analysis for the higher end $\beta(t)$ is analogous. Our analysis is limited to values of $\alpha(t)$ to $0 \leq \alpha(t) \leq (\theta_+ - \theta_-)/2$, which ensures the regulated temperature stays within end-user comfort margins with a maximum reduction in deadband width to half the original width. This limit places an upper bound on the frequency of compressors' on/off cycling, which increases as the hysteresis deadband is narrowed. An overly narrow hysteresis deadband may induce cycling frequencies detrimental to AC compressors. For other TCLs, such as electric water heaters, however, such limits may be more flexible.

3. MODEL FOR AGGREGATE DEMAND RESPONSE TO THERMOSTAT DEADBAND WIDTH CHANGES

This section develops a compact mathematical model of the dynamic aggregate demand response of a population of ACs to a simultaneous step reduction in their hysteresis deadband widths. This model, aimed to be used in model-based DLC design, provides a dynamic mapping between the control input $\alpha(t)$ and the resulting normalised demand of the population $D(t)$.

We follow the modelling approach used in Perfumo et al. (2012) for the response of the population to a step in temperature set-point, in this paper adapted to the response to a step in the lower end of the hysteresis deadband $\alpha(t)$.

We make the following assumptions (Perfumo et al., 2012):

- H.1 All the ACs have the same set-point temperature $\theta_r = (\theta_- + \alpha + \theta_+)/2$ and the same hysteresis deadband width $\theta_+ - \theta_- - \alpha$, where $0 \leq \alpha \leq (\theta_+ - \theta_-)/2$.
- H.2 The ACs operate independently of each other according to the dynamics (1), (2), with parameter C (thermal capacitance) log-normally distributed in the population. The parameters R and P are the same for all the ACs in the population.
- H.3 Each AC operates at 50% duty cycle, which implies that $RP = 2(\theta_a - \theta_r)$ for each device.
- H.4 The regulated temperature swing is much smaller than the difference between ambient and set-point temperatures: $\theta_+ - \theta_- \ll |\theta_a - \theta_r|$. This implies that the rate at which the temperature changes in each AC is approximately constant, so that the temperature shows a triangular waveform.
- H.5 The population demand is at steady state, with temperatures uniformly distributed in the interval $[\theta_-, \theta_+]$ before the step change α is applied.

While in rigour these assumptions clearly restrict the system under consideration, the resulting model tolerates their relaxation to a high degree, as we will illustrate below by simulation. This makes the proposed model appealing for robust model-based DLC design—see Perfumo et al. (2013) for a comprehensive sensitivity analysis of the model developed in Perfumo et al. (2012).

The following lemma gives a characterisation of the population normalised aggregate demand response $D(t)$ as the probability that a randomly chosen AC in the population is turned ON at a given time. The motivating idea behind such probabilistic characterisation (already used in Malhame and Chong, 1985) is that for a sufficiently large distributed population, such probability approximates the proportion of ACs with compressors switched ON at a given time, which corresponds to the normalised demand $D(s)$ defined in (3).

To state this lemma introduce the variable

$$x_i(t) \triangleq \int |\dot{\theta}_i(t)| dt,$$

which under Assumption H.4 may be expressed as

$$x_i(t) \approx x_i^0 + v_i t, \tag{4}$$

In (4) the initial condition x_i^0 is a function of the temperature of the i-th AC, $\theta_i(0)$ at time $t = 0$, and v_i is the rate at which the temperature θ_i changes. By virtue of H.4, such rate is approximated by a constant as

$$|\dot{\theta}_i(t)| \approx v_i = (\theta_a - \theta_r)/C_i R. \tag{5}$$

The variable $x_i(t)$ may be seen as an "unwrapped" map of the temperature $\theta_i(t)$, which converts the triangular waveform into a ramp.

Assuming that the population is sufficiently large, from (5) we now extend such "unwrapped" temperature to a continuous random process, namely,

$$x(t) = x^0 + vt,$$

where x^0 and $v = (\theta_a - \theta_r)/CR$ are now random variables that describe the distribution of initial temperatures and temperature rates in the population. It may be shown (as in Perfumo et al., 2012) that under Assumptions H.1-H.5 v is log-normally distributed with mean μ_v and standard deviation σ_v that satisfy

$$\sigma_{rel} = \frac{\sigma_v}{\mu_v} = \frac{\sigma_C}{\mu_C}. \tag{6}$$

Lemma 1. (Probabilistic model for $D(t)$). Consider a sufficiently large population of ACs operating in steady state under Assumptions H.1 to H.5. Suppose that at time $t = 0$ the lower temperature boundary of the hysteresis deadbands of all ACs in the population are simultaneously raised by α [°C]. Then, the normalised aggregate demand response $D(t)$ for $t > 0$ may be approximated by

$$D(t) \approx \frac{1-\alpha}{2(1+\alpha)} \left(1 + \operatorname{erf}\left[\frac{\log\left[(1-\alpha)/\mu_x(t)\right]}{\sqrt{2}\sigma_{rel}}\right]\right) + \frac{1}{2}\sum_{k=2}^{\infty}(-1)^{k+1} \operatorname{erf}\left[\frac{\log\left[(k(1-\alpha))/\mu_x(t)\right]}{\sqrt{2}\sigma_{rel}}\right], \tag{7}$$

where $\operatorname{erf}[\cdot]$ is the Gauss error function, and $\mu_x(t) = \mu_x(0) + \mu_v t$ is the mean of the values $x(t)$ and σ_{rel} is given by (6).

Proof. The proof follows by adapting the proof of Corollary 1 in Perfumo et al. (2012) from an initial distribution for a deadband width modified by $1 - \alpha$.

Lemma 1 differs from its correlate in Perfumo et al. (2012, Corollary 1) in the dependency on the candidate control variable α in (7). Corollary 1 in Perfumo et al. (2012) showed that the transients in $D(t)$ due to a step change in temperature set-points display oscillations with period $T \approx 2/\mu_v$, assuming deadbands with unitary width, $H = 1$. Following similar steps, it may be shown from Lemma 1 that the period of the oscillations in $D(t)$ due to a step reduction α°C in hysteresis deadband width is also a function of α in the present case, namely,

$$T \approx 2H/\mu_v = 2(1-\alpha)/\mu_v. \tag{8}$$

Equation (8) indicates the presence of a nonlinearity in the response $D(t)$ with respect to the input α. This nonlinear dependency is explicit in the following second-order analytic model approximation of $D(t)$, which is the main result of the paper.

Proposition 2. (A second-order model for $D(t)$). Under the assumptions of Lemma 1, the aggregate demand response $D(t)$ of a population of ACs to a step change α°C in the lower boundary of the hysteresis deadband is approximated by the output $y(t)$ of the second-order system

$$\dot{x}_1 = -2f_1(\alpha)x_1 - f_2(\alpha)x_2 + \alpha, \qquad (9)$$
$$\dot{x}_2 = x_1,$$
$$y(t) = h\big(g_1(\alpha)x_1 + g_2(\alpha)x_2\big) + (1-\alpha)D_{ss}(\theta_r, 1), \qquad (10)$$

where $h(\cdot)$ is the saturation function $h(z) = 0$, if $z \geq 0$ and $h(z) = -z$ otherwise, and

$$f_1(\alpha) = \frac{\mu_v|\log(r(\alpha))|}{1-\alpha}; f_2(\alpha) = f_1(\alpha)^2 + \mu_v^2\pi^2/(1-\alpha)^2$$
$$\frac{g_2(\alpha)}{f_2(\alpha)} = \frac{[(1-\alpha)D_{ss}(\theta_r,1) - D_{ss}(\theta_r + 0.5\alpha, 1-\alpha)]}{\alpha};$$
$$g_1(\alpha) = \Big[f_1(\alpha) - \pi\mu_v/\big((1-\alpha)\sqrt{r(\alpha)}\big)\Big]\, g_2(\alpha)/f_2(\alpha),$$
$$r(\alpha) = \frac{|\operatorname{erf}\left(\frac{1-\alpha}{1-\alpha+(2-\alpha)\sqrt{2}\sigma_{rel}}\right) - \frac{1}{2}|}{|\operatorname{erf}\left(\frac{1-\alpha}{1-\alpha+\alpha\sqrt{2}\sigma_{rel}}\right) - \frac{1}{2}|},$$
$$\mu_v = (\theta_a - \theta_r)(1+\sigma_{rel}^2)/R\mu_C, \quad \text{and}$$
$$D_{ss}(\theta, H) = \left(1 + \frac{\log(1 + \frac{H}{\theta_a - \theta - H/2})}{\log(1 + \frac{H}{PR + \theta - \theta_a - H/2})}\right)^{-1}.$$

Proof. Due to space limitations we omit the proof, which follows that for (Perfumo et al., 2012, Corollary 2), but using the envelope bound for $D(t)$ in Lemma 1. □

Proposition 2 characterises the aggregate demand response of a population of ACs as the dynamic response of a second-order time-invariant model parametrized by the population distributed physical parameters. As in the case of control by set-point offsets (Perfumo et al., 2012), such low-order model for aggregate demand dynamics may be used very effectively for transient analysis and model-based DLC design (Braslavsky et al., 2013).

For example, for a fixed value of α the model (9) is an underdamped linear system with characteristic polynomial $s^2 + 2\xi(\alpha)\omega(\alpha)s + \omega^2(\alpha)$. The duration of transients in aggregate demand response to a step reduction α in deadband width may then be estimated using the well-known rule-of-thumb formula for the settling time in the steps response of a second order LTI system (e.g., Franklin et al., 2006 §3.4.3)

$$t_s(\alpha) = 4.6/\xi(\alpha)\omega(\alpha), \qquad (11)$$

where here the damping ratio $\xi(\alpha) = f_1(\alpha)/\omega(\alpha)$ and underdamped natural frequency $\omega(\alpha) = \sqrt{f_2(\alpha)}$ are parametrized by the size of the step α — a main difference with the response to steps in temperature set-point (Perfumo et al., 2012, Corollary 2), where they are invariant.

Table 2 shows the values assumed by the nonlinear coefficients of the model used to obtain the responses shown in Figure 1. This Figure shows the response of the model computed from Proposition 2 for two values of α together with the corresponding simulated responses of 10,000 ACs, each independently operating according to (1), (2), and with physical parameters distributed as shown in Table 1. We can see how closely the computed model can capture the dominant dynamics in the simulated aggregate response. Using (11) and the values computed on Table 2 we can estimate the settling times of the responses shown in Figure 1 as $t_s = 418$ for $\alpha = 0.1$, and $t_s = 219$ for $\alpha = 0.4$, which are in very close agreement with those of the simulated transients in the plots.

Table 2. Values of the nonlinear functions $f_1(\alpha), f_2(\alpha), g_1(\alpha)$ and $g_2(\alpha)$ in Proposition 2 to generate the responses in Figure 1.

α	$f_1(\alpha)$	$f_2(\alpha)$	$g_1(\alpha)$	$g_2(\alpha)$	d
0.1	0.011	0.0013	0.021	-6×10^{-4}	0.5
0.4	0.021	0.0032	0.035	-14×10^{-4}	0.5

Note that the responses simulated using (1), (2) are *not* restricted by Assumptions H.1 to H.5 used to derive the model (e.g., all R, P and C are distributed), which illustrates the robustness of the model in Proposition 2. Also, as may be checked, the nonlinearities on α in the model given by Proposition 2 are smooth and have limited range for the domain of values of α considered, which makes the proposed model amenable to a range of practical model-based control design techniques, such as linearised and gain-scheduling feedback designs (e.g., Khalil, 2002).

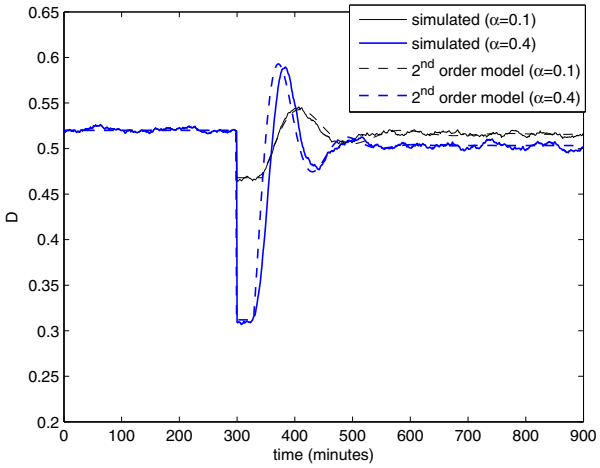

Fig. 1. Normalised power demand D for 10,000 simulated ACs vs. model $y(t)$ in (9)-(10) for $\alpha = 0.1$ and $\alpha = 0.4$.

A special characteristic of the responses to steps in $\alpha(t)$ observed in Figure 1 is that immediately after the step there is a period where the demand stays constant for a period of time. This is not observed in the responses to steps to set-point offsets, where aggregate demand drops instantaneously and then continues to gradually drop until it reaches a minimum (Perfumo et al., 2012).

These initial flat periods in the responses to steps in $\alpha(t)$ may be explained by analysing the distribution of temperatures of on and OFF ACs before and immediately after the step, which are schematically shown in Figure 2. Figure 2(a) (before the step) shows the population in steady state with ON and OFF ACs uniformly distributed along the regulation deadband. Figure 2(b) shows the distribution of ON and OFF ACs immediately after the step. We can see that all the ACs with temperatures smaller than $\theta_- + \alpha$ at the step time simultaneously turn OFF, which causes an instantaneous drop in demand. For a period of time the number of ACs turning ON balances that of ACs turning OFF, which explains the constant period after the step. This period ends when the vertical arm of the "L" shaped histogram of OFF ACs reaches the upper deadband limit θ_+, at which point there will be more

ACs turning ON than turning OFF, and hence the demand will start to rise. Note that as time goes by, the OFF histogram in Figure 2(b) will lose its "boxed L" shape, as the heterogeneity in the population causes the histograms to converge to their steady- state distribution (which is why we observe *decaying* oscillations in the response).

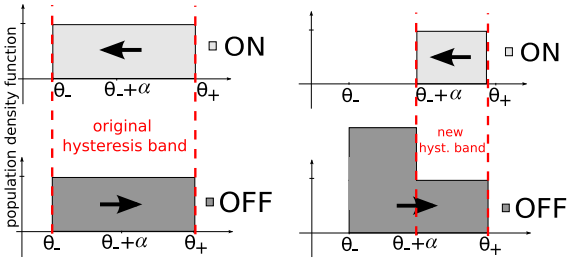

(a) Before step (b) After step

Fig. 2. Temperature distribution before and after a step in α to narrow deadband from $[\theta_-, \theta_+]$ to $[\theta_- + \alpha, \theta_+]$.

We follow this analysis to obtain a theoretical upper bound for the maximum amount of energy that may be released by manipulating aggregate demand through offsets in α.

4. THEORETICAL UPPER BOUND ON THE MAXIMUM AMOUNT OF RELEASED ENERGY

As mentioned earlier, manipulation of α can only shape a limited amount of aggregate energy for a given population. We now obtain an analytic quantification of such maximum energy limit. This upper bound is obtained by considering the case of a homogeneous population of ACs, namely, consisting of all identical devices

Our analysis focuses on the distributions of on/off ACs immediately after the step change in α. Such distributions are illustrated in Fig. 2(b) over temperatures, and in Fig. 3 over the "unwrapped" temperature $x(t)$. If $D_{ss}(\theta_{ref})$ represents the steady state value of the aggregate demand response before the step change, we see that the demand instantaneously drops to $(1-\alpha)D_{ss}(\theta_{ref})$ since only $(1-\alpha)\%$ of the ACs are on. Subsequently, the same number of ACs turn ON and OFF until the tall part of the "L" shaped histogram of OFF ACs reaches $2(1-\alpha)$, which causes the flat period in the aggregate demand response after the initial instantaneous drop, as seen in Figure 1.

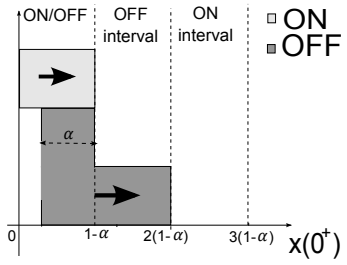

Fig. 3. Distribution of $x(0^+)$ (following a step change at $t = 0$ in lower temperature of hysteresis deadband).

In an ideal homogeneous population, the histogram of Fig. 3 keeps its shape and moves to the right with the constant speed of μ_v, which makes this flat period equal to

$$T_0 = (1-\alpha)/\mu_v. \tag{12}$$

As the tall part of the "L" shaped histogram of OFF ACs enters into the ON interval $[2(1-\alpha), 3(1-\alpha)]$, the demand linearly rises until it completely located within that interval. The rising time for the ideal homogeneous population equals to α/μ_v. The demand stays at this maximum for a time $(1-2\alpha)/\mu_v$, until the tall part of the "L" shaped histogram of OFF ACs enters into the OFF interval $[3(1-\alpha), 4(1-\alpha)]$, which causes the linear reduction in the demand. Such kind of oscillation continues with period of $2(1-\alpha)/\mu_v$ as in (8) and should be centred around the final steady state value of $D_{ss}(\theta_{ref} + \alpha/2)$. Therefore, the maximum value of the aggregate demand in the homogeneous population is

$$D_{max} = 2D_{ss}(\theta_{ref} + 0.5\alpha, 1-\alpha) - (1-\alpha)D_{ss}(\theta_{ref}, 1).$$

A schematic demand response of an ideal homogeneous population schematically plotted in Fig. 4.

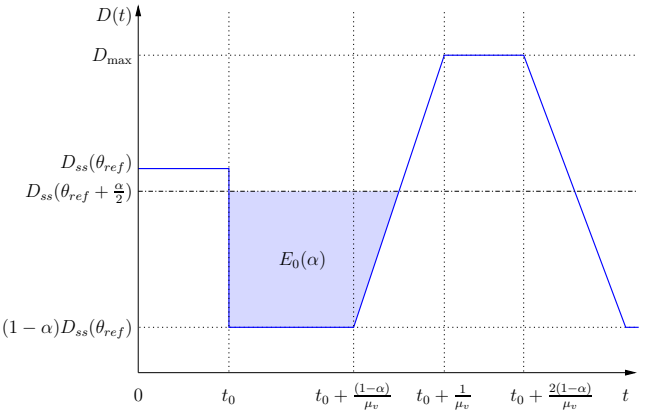

Fig. 4. Typical aggregate power demand response of an ideal homogeneous population for $\alpha \in [0, 0.5]$.

To compare the released energy for different populations, we compute the total amount of released energy as

$$E(t;\alpha) = E_{\sigma_{rel}}(\alpha) + \Delta D\, t, \tag{13}$$

where $E_{\sigma_{rel}}(\alpha)$ is the whole amount of released energy with respect to the steady state value of $D_{ss}(\theta_{ref} + \alpha/2)$ and $\Delta D = D_{ss}(\theta_{ref}, 1) - D_{ss}(\theta_{ref} + 0.5\alpha, 1-\alpha)$ for a distributed population characterised by σ_{rel}, for a given value of α. Equation (13) allows us to quantify the amount of energy released in a way that does not diverges with time, as would occur if the integration were done with respect to the initial value before applying the step, i.e., $D_{ss}(\theta_{ref}, 1)$ since $D_{ss}(\theta_{ref} + 0.5\alpha, 1-\alpha) < D_{ss}(\theta_{ref}, 1)$.

Since $\Delta D\, t$ in (13) is invariant for different populations, we only need the first term for comparison. For an ideal homogeneous population, E_0 is the surface of the shaded trapezoid shown in Fig. 4 and may be computed as

$$E_0(\alpha) = \left((4-3\alpha)[\alpha D_{ss}(\theta_{ref}, 1) - \Delta D]\right)/4\mu_v. \tag{14}$$

In a heterogeneous population, the histogram in Fig. 3 loses its polygon shape as time evolves, which causes the demand response to smoothly oscillate and eventually settle down to a new steady-state value $D_{ss}(\theta_{ref} + \alpha/2)$. Fig. 5 plots equation (14) per AC (thin blue line) as well as the simulated values for the populations of ACs with different levels of heterogeneity. It appears that the homogeneous response is an upper bound for all cases and

the less the heterogeneity of the population, the less the distance to the computed upper bound.

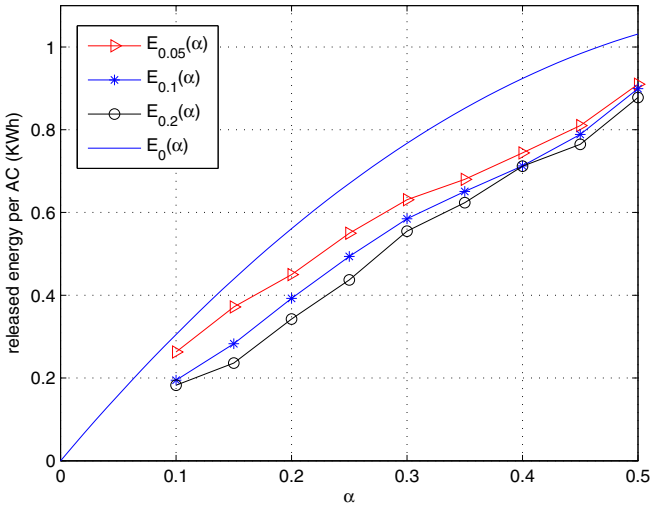

Fig. 5. Theoretical normalised upper bound (14) per AC with $P = 6KW$ versus simulated $E_{\sigma_{rel}}(\alpha)$ for $\sigma_{rel} = 0.05, 0.1, 0.2$, when $\mu_v = 0.83$ and $D_{ss}(\theta_{ref}, 1) = 0.5$ based on the parameters in Table 1.

The analysis done in this section illustrates how one could quickly determine the potential kW and kWh that a population could deliver by DLC by deadband width manipulation. For example, for a population of 1,000 houses with physical characteristics as per Table 1 and a coefficient of performance value of 2.5, the maximum power that could be released for $\alpha = 0.5$ is 600 kW and during the first trough in the oscillations (which lasts for about an hour), and we can deliver at most 400 kWh.

5. CONCLUSIONS

Manipulating the hysteresis boundaries of air conditioners allows to alter their power profile without violating defined end-use comfort constraints. We have developed a second-order model of the power response of a population of air conditioners to a common step change in one of the boundaries of the hysteresis band. Simulation results indicate that our model successfully captures this response.

Interestingly, the parameters of our proposed model analytically depend not only on the physical characteristics of the population, but also on the value of the step change in deadband width. This dependency, however, is well-behaved and amenable by a range of control design techniques. This means that the new control input α can be used to shape the aggregated power demand transient response and hence, could be a good candidate for DLC.

The proposed model requires knowledge of the distributions of physical parameters in the population, which could be obtained from statistical surveys, or inferred using the proposed model structure and measured data. The latter is under current development by the authors.

A caveat of the proposed DLC approach is that it inherently changes the compressor cycling, which may be detrimental to the equipment if taken to an overly high frequency. It could be argued that demand response events only happen occasionally and thus the impact of the life cycle of the compressor would be small, although experiments should be carried to assess this impact more precisely.

The relative simplicity of the proposed model makes it practical in model-based DLC design. The resulting control strategy, which can manipulate power without comfort penalties, offers new avenues to overcome one of the main obstacles for using air conditioners for demand response: end-user impact.

REFERENCES

S. Bashash and H.K. Fathy. Modeling and control of aggregate air conditioning loads for robust renewable power management. *IEEE Trans. on Control Systems Technology*, 21(4):1318–1327, 2013.

J. H. Braslavsky, C. Perfumo, and J. K. Ward. Model-based feedback control of distributed air-conditioning loads for fast demand-side ancillary services. In *Proc. of the 52nd IEEE Conference on Decision and Control*, pages 6274–6279, Florence, Italy, December 2013.

D. S. Callaway. Tapping the energy storage potential in electric loads to deliver load following and regulation, with application to wind energy. *Energy Conversion and Management*, 50(5):1389–1400, 2009.

D.S. Callaway and I.A. Hiskens. Achieving controllability of electric loads. *Proc. of the IEEE*, 99(1):184–199, 2011.

G. Franklin, D. Powell, and A. Emami-Naeini. *Feedback Control of Dynamic Systems*. Prentice Hall, 2006.

L. Hughes. Meeting residential space heating demand with wind-generated electricity. *Renewable Energy*, 35(8): 1756–1772, 2010.

S. Ihara and F.C. Schweppe. Physically based modeling of cold load pickup. *IEEE Trans. on Power Apparatus and Systems*, PAS-100(9):4142 –4150, September 1981.

H. Khalil. *Nonlinear systems*. Prentice Hall, 2002.

J. Li, G. Poulton, and G. James. Coordination of distributed energy resource agents. *Appl. Artif. Intell.*, 24 (5):351–380, May 2010.

R.P. Malhame and C. Chong. Electric load model synthesis by diffusion approximation of a high-order hybrid-state stochastic system. *IEEE Trans. on Automatic Control*, 30(9):854 – 860, sep. 1985.

J.L. Mathieu, S. Koch, and D.S. Callaway. State estimation and control of electric loads to manage real-time energy imbalance. *IEEE Trans. on Power Systems*, 28 (1):430–440, 2013.

C. Perfumo, E. Kofman, J. H. Braslavsky, and J. K. Ward. Load management: Model-based control of aggregate power for populations of thermostatically controlled loads. *Energy Conversion and Management*, 55:36–48, 2012.

C. Perfumo, J. H. Braslavsky, and J. K. Ward. A sensitivity analysis of the dynamics of a population of thermostatically-controlled loads. In *Proc. of the Australasian Universities Power Engineering Conference (AUPEC)*, Hobart, September 2013.

W. Zhang, J. Lian, C. . Chang, and K. Kalsi. Aggregated modeling and control of air conditioning loads for demand response. *IEEE Trans. on Power Systems*, 28(4): 4655–4664, 2013.